Kirkuk Journal of Science Vol. 20, Iss. 1, p. 35-42, 2025 doi:10.32894/kujss.2025.157914.1196

Electron Scattering Form Factors of ^{92}Mo in the Shell Model Framework: Incorporating Core-Polarization Effects

Sarah M. Obaid *

Department of Medical Physics, College of Science, Al-Mustaqbal University, Babylon, Iraq.

*Corresponding author : sarah.mahdi@uomus.edu.iq

Article Information

Article Type:
Research Article

Keywords:
C2 and C4 form factors; E3 E5 E7 form factors; Tassie model; Skyrme potential; Core polarization.

History:
Received: 3 February 2025
Revised: 10 March 2025
Accepted: 18 March 2025
Available Online: 25 March 2025

Citation: Sarah M. Obaid, Electron Scattering Form Factors of ^{92}Mo in the Shell Model Framework: Incorporating Core-Polarization Effects, Kirkuk Journal of Science, 20(1), p. 35-42, 2025, https://doi.org/10.32894/kujss.2025.157914.1196

Abstract

Shell model calculations have been used to study the Coulomb C2, C4, and transverse E3, E5, and E7 form factors, including core-polarization effects in the 2^+, 3^-, 4^+, 5^- and 7^- states of ^{29}Mo. The computations were done using the two-body effective interaction n50j with the model space n50j. The Coulomb Valence Tassie Model (CVTM), which takes into consideration excitations outside of the model space, was used to assess core-polarization effects. The Skyrme potential was used to calculate the wave functions of the radial single-particle matrix elements, which gave a realistic description of nuclear interactions. Core-polarization effects are crucial for effectively improving the form factor calculations because they greatly increase agreement with the available experimental data.

1. Introduction:

Nuclear forces and the fundamental principles regulating particle interactions may be fundamentally understood through the scattering of distinct particles by different objects [1]. One of the best techniques for examining nuclear structure among these approaches is high-energy electron scattering, which provides important information on the characteristics of atomic nuclei. Because electrons may interact with nuclei electromagnetically instead of by the strong nuclear force, they are perfect probes for studying magnetic moments, transition densities, and nuclear charge distributions.

Determining nuclear charge radii and the radial distribution of charge within nuclei has been one of the most important contributions of electron scattering experiments [2]. In addition to verifying that nuclei have a relatively uniform charge density in their core with a progressive falloff at the surface, these studies have provided extensive information on the size and structure of different isotopes [3]. Furthermore, the current and magnetic densities involved in nuclear transitions have been revealed thanks in large part to electron scattering, which has produced vital information for improving nuclear models [4].

The transition matrix components of the local charge and current density operators, which contain important details about the internal structure of the target nucleus, are closely connected to the cross-section of electron scattering [5]. Researchers may derive accurate information regarding nuclear deformation, collective excitations, and single-particle dynamics by examining differential cross-sections and form factors [6]. Additionally, electron scattering investigations have greatly advanced our knowledge of the nature of short-range nucleon-nucleon interactions, the function of meson-exchange currents, and nuclear shell structure [7].

In addition to nuclear structure research, parity-violating electron scattering experiments have been used to test basic symmetries and investigate the function of weird quarks in nucleon structure. High-precision electron scattering is still a vital tool in nuclear physics as experimental methods develop, providing fresh perspectives on the nature of strong interactions and the basic makeup of matter [8].

Majeed et al., have addressed that the core polarization effects within a microscopic theoretical treatment should be considered for form factor calculations. In this case, it is necessary to explicitly take into account the excitation of core nucleons into the model space, where focus is given to exciton energies $2\hbar\omega$ and $4\hbar\omega$. The calculations performed for different nuclei, including those from the p, sd and fp shells, have achieved quite remarkable success in reproducing measured form factors, which is an indirect measure of the effectiveness of core polarization phenomenon that is necessary to capture the reality of the nuclear structure. This paper demonstrates the validity of the selected theoretical approach and serves to explain the intricate interactions between the nucleons of the nucleus [9], [10], [11], [12], [13]. Majeed has previously shown that core polarization must be accounted for by either adding effective charges for protons and neutrons or by incorporating it via microscopic theory.

In the context of the shell model, Majeed and Obaid examined the inelastic electron scattering for longitudinal and transverse form factors of ^{65}Cu and ^{71}Ga nuclei that are located in the fp-shell area. Using the jun45 effective interaction, the computation is carried out in the ($1f_{5/2}$, $2p_{3/2}$, $2p1/2$, $1g_{9/2}$) model space [14].

This study aims to examine the electron scattering form factors for certain states of ^{92}Mo, integrating core polarization effects within the Coulomb Valence Tassie Model (CVTM). The shell model code NushellX@MSU is used to investigate the computations, and the correctness and dependability of the findings are evaluated by methodically comparing them with the available experimental data.

2. Theoretical Background:

Using the Bohr-Mottelson equations, the effective proton and neutron charges are calculated [15]:

$$e_{eff}(t_z) = e(t_z) + e\delta e(t_z)$$
$$e\delta e(t_z) = Z/A - 0.32(N-Z)/A - 2tz[0.32 - 0.3(N-Z)A] \tag{1}$$

$$where \;\; t_z(p) = 1/2 \; and \; t_z(n) = -1/2$$

One-body density matrix (OBDM) components and reduced single-particle matrix elements are combined to create the reduced matrix element of the electron. For a multipolarity n-particle model space wave function, the scattering operator is shown as [16]:

$$\langle f \| \hat{o}^{\lambda} \| i \rangle = \sum_{ab} OBDM(f,i,a,b,\lambda) \langle f \| \hat{o}^{\lambda} \| i \rangle \tag{2}$$

$$\langle f \| \hat{o}\lambda \| i \rangle = \langle f \| \hat{o}^{MS} \| i > + \langle f \| \hat{o}^{CP} \| i \rangle \tag{3}$$

where the core-polarization (CP) and model space (MS) matrix elements in Eq. 3 are provided as [14].
In Eq. 3, the matrix elements of the core-polarization (CP) and the model space (MS) are provided as [16].

$$\langle f \| \hat{o}^{MS} \| i \rangle = q \int_0^{\infty} drr^2 j_{\lambda}(qr) \rho^{MS}_{\lambda,u}(r) \tag{4}$$

$$\langle f \| \hat{o}^{CP} \| i \rangle = \int_0^{\infty} drr^2 j_{\lambda}(qr) \triangle \rho^{CP}_{\lambda,u}(r) \tag{5}$$

In terms of transition charge density, the matrix element of Coulomb interaction is represented by the sum of the (MS) and (CP) components [16]:

$$O(C\lambda, q) = q \int_0^{\infty} drr^2 j_{\lambda}(qr) \rho^{MS}_{\lambda,p}(r) + \int_0^{\infty} drr^2 j_{\lambda}(qr) \triangle \rho_{\lambda}(r) \tag{6}$$

The charge density $\rho^{MS}_{\lambda,p}(r)$ of the nucleons with a spherical Bessel function for j_{λ} (qr) and a momentum transfer of q, the one-body density matrix is used to define the MS(r) of the transition for the initial (i) and final (f) nuclear states [16]:

$$\rho^{MS}_{\lambda,u}(r) = \sum_{k_a,k_b}^{MS} F(i,f,k_a,k_b,\lambda,u) \langle j_a \| Y_{\lambda} \| j_b \rangle R_{n_a l_a}(r) \tag{7}$$

The one body matrix element F(i, f, k_a, k_b, λ, u) and the single-particle (s.p.) states (nlj) are based on k. The index (u) refers to either protons or neutrons. The following represents the CP valence model (V) density of transition [16]:

$$\triangle \rho^{V}_{\lambda}(r) = \delta e_p \rho^{MS}_{\lambda,p} + \lambda e_n \rho^{MS}_{\lambda,n} \tag{8}$$

Polarization is explained by the charges associated with protons (δe_p) and neutrons (δe_n). For Tassie model transition density the CP is represented by [16]:

$$\triangle\rho^{T}_{\lambda,p}(r) \propto r^{\lambda-1}\frac{d\rho^{core+Ms}_{0,p}(r)}{dr} = Nr^{\lambda-1}\frac{d\rho^{core+Ms}_{0,p}(r)}{dr} \tag{9}$$

The charge density of the ground state is [16]:

$$\begin{aligned} d\rho^{core+Ms}_{0,p}(r) = &\sum_{k_a,k_b}^{Core+MS} F(i,f,k_a,k_b,0,p) \\ &\times \langle j_a\|\lambda Y_0\|j_b\rangle R_{n_a l_a}(r) R_{n_b l_b}(r) \end{aligned} \tag{10}$$

the proportionality constant N (at the photon point) is given by the gamma transitions matrix elements M (E λ), q = E$_\gamma$ /$\hbar$c, where E$_\gamma$ is the energy due to excitation [16], [17]:

$$\begin{aligned} M(E\lambda) =&\{e\int_0^\infty drr^2 r^\lambda(qr)\rho^{MS}_{\lambda,p}(r) \\ &+N\int_0^\infty drr^2 r^{\lambda+1}(qr)\rho^{MS}_{\lambda,n}(r)\} \end{aligned} \tag{11}$$

It is possible to describe the elements of the gamma transition matrix as elements of the MS matrix with effective charges [18]

$$\begin{aligned} M(E\lambda) =&e^{eff}_p\int_0^\infty drr^2 r^\lambda(qr)\rho^{MS}_{\lambda,p}(r) \\ &+e^{eff}_n\int_0^\infty drr^2 r^\lambda(1qr)\rho^{MS}_{\lambda,n}(r) \end{aligned} \tag{12}$$

By using the effective charges, N, the constant of proportionality, is obtained by combining Eq. 11 and Eq. 12. These aforementioned models for effective neutrons and protons are discussed in depth in Ref. [17], [18].

The electron scattering form factor for shell model of nuclear states between initial (i) and final (f), comprising angular momentum and momentum transfer q, is expressed as [17], [18]:

$$|F_{\eta\lambda}(q)|^2 = \frac{4\pi}{Z^2}\frac{1}{2j_i+1}|O(C\lambda,q)|^2|F_{cm}(q)F_{js}(q)|^2 \tag{13}$$

Utilizing longitudinal Coulomb (C) and transverse electric (E) and magnetic (M) form factors, the center of mass correction is expressed as F_cm (q) = $\frac{e^{q^2b^2}}{4A}$, attributed to the absence of transitional invariance in the shell model, and F$_{fs}$(q) = [1+ $(\frac{q}{4.33})^2]^{-2}$.

3. Results and Discussion:

The computations, discussion, and comparison of the anticipated outcomes with the measured data will take up this section. In addition to the method of fitting the two-body matrix elements to the observed data from the work of Ref. [19] to describe the charge density and form factors, there are other theoretical attempts to explain the properties of fp-shell nuclei, the model space used, and the involved parameters.

According to the traditional shell model, the core is taken at ^{78}Ni for ^{29}Mo nucleus with nucleons scattered across 2p$_{3/2}$, 1f$_{5/2}$, 2p$_{1/2}$, 1g$_{9/2}$ shells. The model space is n50j and the skyrme interaction was used for form factor calculations.

This research implements core polarization adjustments in the Coulomb Valence Tassie Model (CVTM) framework and uses the Skyrme potential to improve nuclear structure estimates for electron scattering form factors. Our research uses the n50j model space and the NushellX@MSU computational framework to tackle core polarization effects more comprehensively and systematically than previous techniques. The selection of effective charges and parameter optimization improves experimental data agreement, emphasizing the need for higher-order adjustments. This study's improved computational precision and shell-model interaction treatment shed light on ^{92}Mo nuclear structure and prepare for future extensions with many-body effects and relativistic corrections.

3.1 Positive Parity States:

Figure 1 compares actual data (black dots) with two theoretical models: ”ms only” (blue curve) and ”ms+CP” (red curve) to show the Coulomb form factor $|FC2(q)|^2$ for the 2^+_1 state (1.509 MeV) in ^{92}Mo. The y-axis is logarithmic, emphasizing the rhythmic pattern typical of nuclear structure effects, while the x-axis depicts the momentum transfer q (fm^{-1}). The first peak represents the primary transition strength at around 0.4 fm^{-1}, and the charge distribution and interference effects are reflected in the oscillations that follow. Compared to the blue curve, which alone takes monopole strength (ms) into account, the red curve, which takes core polarization (CP) into account, more closely matches experimental data, highlighting the need for CP corrections in theoretical modeling. Variations at higher q might indicate experimental errors or the absence of higher-order effects.

Figure 2 depicts the squared electron scattering form factor $|FC4(q)|^2$ for the initial 2^+_2 excited state of ^{92}Mo at 3.096 MeV as a function of momentum transfer q. The black dots signify actual data, whilst the blue and red curves illustrate theoretical estimates derived from the shell model, accounting for and excluding core polarization (CP) effects, respectively. The incorporation of core polarization (red curve) improves the concordance with experimental data, especially in repli-

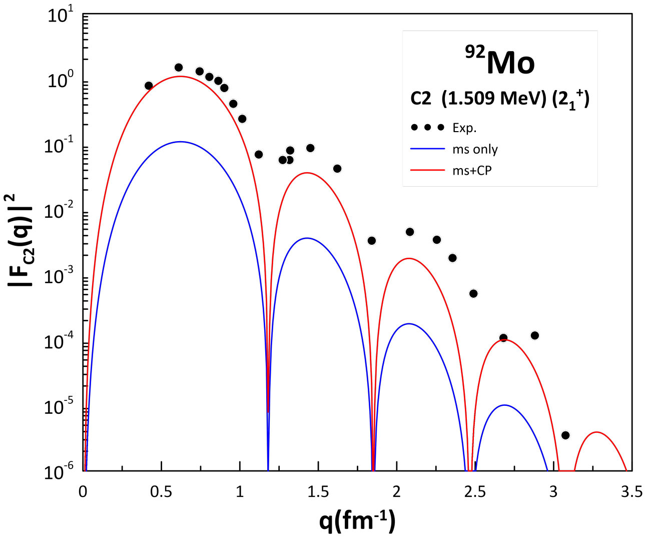

Figure 1. shows the longitudinal C_2 form factor for the 2_1^+ state at 1.509 MeV in ^{92}Mo. The experimental findings [20] (black dots) are compared to shell model calculations: 'ms alone' (blue) without core polarization and 'ms+CP' (red) with core polarization, which demonstrate better agreement when CP effects are included.

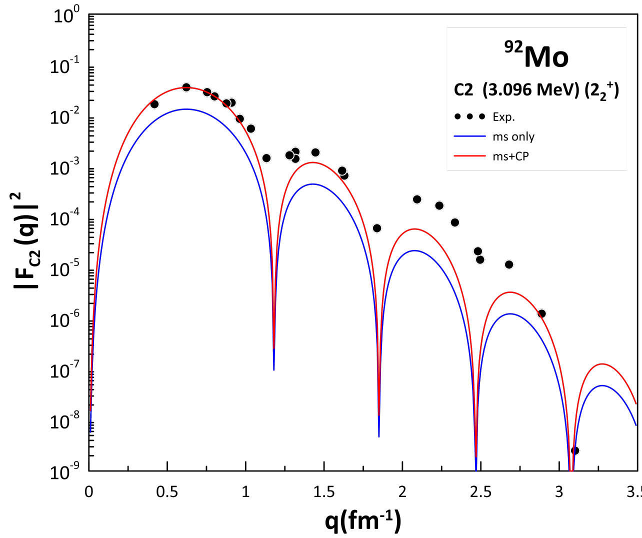

Figure 2. Longitudinal C2 form factor for the 2_2^+ state at 3.096 MeV in ^{92}Mo. Experimental data [20] (black dots) are compared with shell model calculations: 'ms only' (blue) without core polarization and 'ms+CP' (red) with core polarization, showing improved agreement when CP effects are included.

cating peak amplitudes and the general trend, underscoring the importance of core polarization in precisely characterizing nuclear structural effects in electron scattering investigations.

Figure 3 displays the squared electric octupole form factor $|FE3(q)|^2$ for the 3_1^- state (2.850 MeV) of ^{92}Mo, plotted against momentum transfer q. The experimental findings (black dots) are contrasted to the theoretical predictions of two models: "ms only" (blue line) and "ms+CP" (red line). The addition of core polarization (CP) effects improves the model's fit with experimental data, particularly in peak regions. The form factor's rhythmic features disclose the essential nuclear structure, with changes at high q values indicating likely additional contributions that are not well characterized by models.

Figure 4 shows the squared Coulomb form factor $|F(q)|^2$ as a function of momentum transfer q in the 4_1^+ state (2.282 MeV) of ^{92}Mo. The experimental results (black dots) are shown against two theoretical calculations: the "ms only" model (blue line) and the "ms+CP" model (red line). Incorporating CP (core polarization) effects into the "ms+CP" model improves agreement with experimental findings, especially in the peak area at q≈1 fm^{-1}. Both theoretical curves represent the overall trend of the experimental data. The differences at higher q values point to extra nuclear structural effects that may not be completely accounted for in theoretical models.

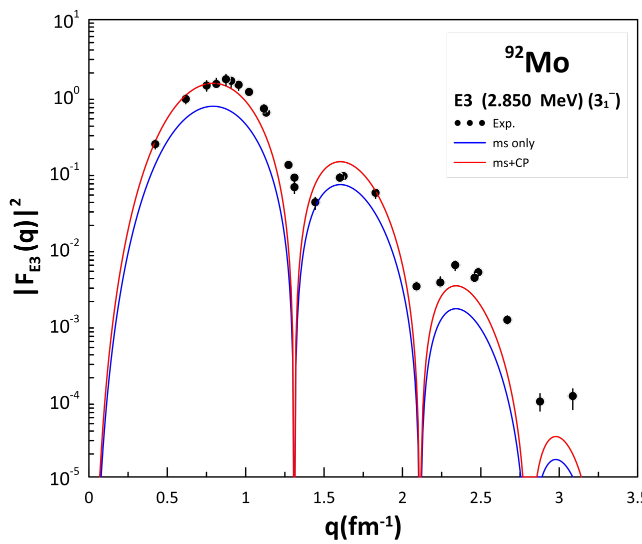

Figure 3. Longitudinal C2 form factor for the 2_2^+ state at 3.096 MeV in ^{92}Mo. Experimental data [20] (black dots) are compared with shell model calculations: 'ms only' (blue) without core polarization and 'ms+CP' (red) with core polarization, showing improved agreement when CP effects are included.

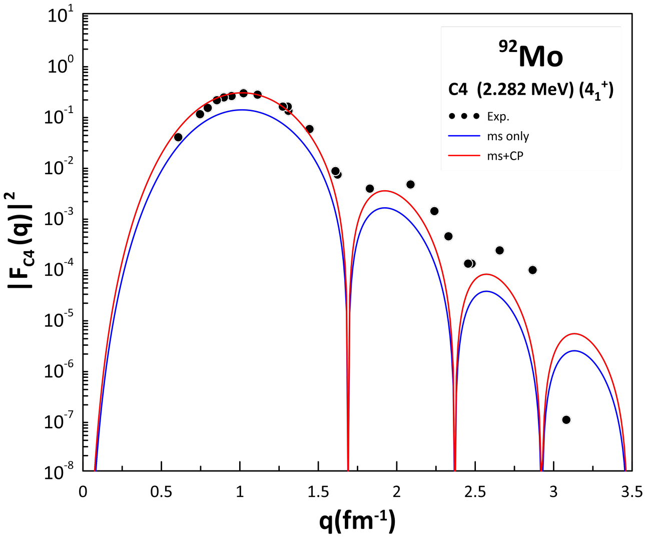

Figure 4. Longitudinal C 4form factor for the 4_1^+ state at 2.282 MeV in ^{92}Mo. Experimental data [20] (black dots) are compared with shell model calculations: 'ms only' (blue) without core polarization and 'ms+CP' (red) with core polarization, showing improved agreement when CP effects are included.

Figure 5 shows the squared Coulomb form factor $|FC4(q)|^2$ for the 4_2^+ state (3.369 MeV) of ^{92}Mo shown as a function of momentum transfer q. The experimental results (black dots) are compared to theoretical calculations using the "ms only" model (blue line) and the "ms+CP" model (red line). Including core polarization (CP) effects in the "ms+CP" model improves form factor predictions, resulting in improved agreement with experimental results, particularly at lower q values. However, certain variations continue at greater q, indicating extra nuclear structural contributions that are not completely addressed by theoretical models.

For the 5_1^- state (2.527 MeV) of ^{92}Mo, the squared electric form factor $|FE5(q)|^2$ is shown in Figure 6 as a function of the momentum transfer q. The blue line represents the "ms only" model, whereas the red line represents the "ms+CP" model. The black dots represent experimental data, while the red line represents theoretical predictions. An improvement in agreement with experimental data is shown in the peak area around q≈1 fm^{-1} when core polarization (CP) effects are included in the "ms+CP" model. Nevertheless, differences persist at greater (q) values, suggesting that contributions from the nuclear structure may be lacking. There seems to be an unnecessary annotation called "High-Low-Close Plot 3" in the legend.

The state 7_1^- at (4.560 MeV) is shown in Figure 7 as the squared electric form factor $|FE7(q)|^2$. Two models the

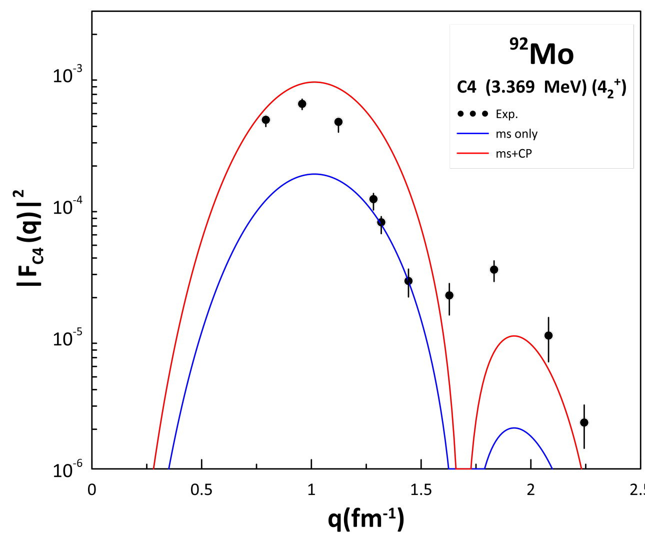

Figure 5. Longitudinal C 4form factor for the 4_1^+ state at 2.282 MeV in ^{92}Mo. Experimental data [20] (black dots) are compared with shell model calculations: 'ms only' (blue) without core polarization and 'ms+CP' (red) with core polarization, showing improved agreement when CP effects are included.

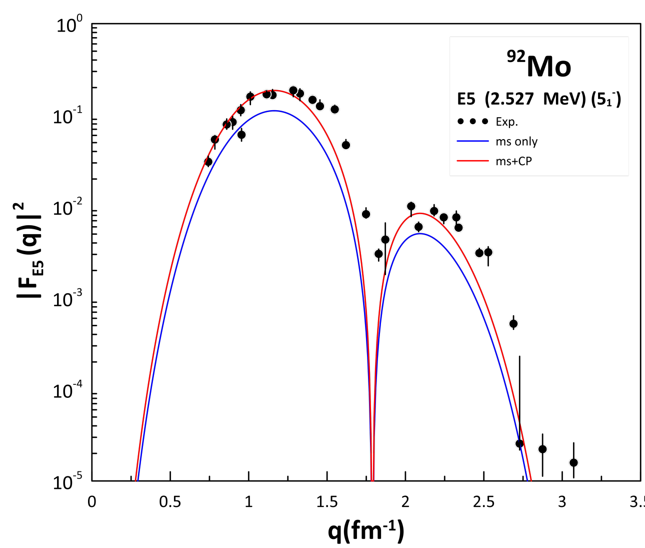

Figure 6. Transverse E_5 form factor for the 5_1^- state at 2.527 MeV in ^{92}Mo. Experimental data [20] (black dots) are compared with shell model calculations: 'ms only' (blue) without core polarization and 'ms+CP' (red) with core polarization, showing improved agreement when CP effects are included.

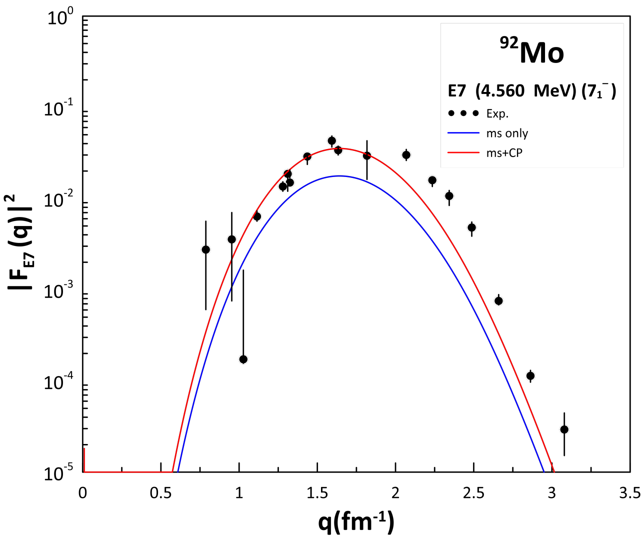

Figure 7. Transverse E_5 form factor for the 5_1^- state at 2.527 MeV in ^{92}Mo. Experimental data [20] (black dots) are compared with shell model calculations: 'ms only' (blue) without core polarization and 'ms+CP' (red) with core polarization, showing improved agreement when CP effects are included.

"ms only" (blue line) and the "ms+CP" (red line) are used to compare experimental results (black dots) with theoretical calculations. Particularly in the peak area at q≈1.5 fm^{-1} include core polarization (CP) effects enhance the agreement of the "ms+CP" model with experimental results. Larger error bars and differences at lower q values might be indicators of experimental errors or extra nuclear structural contributions the theoretical model fails to explain completely.

Although earlier research has examined electron scattering form factors and included core polarization effects [10], [11], [12], [13], [17], this work contributes to the field by incorporating the Skyrme potential and the Coulomb Valence Tassie Model (CVTM) into the shell model framework to improve theoretical prediction accuracy. In contrast to previous methods that often depended on empirical modifications or constrained model spaces, our investigation uses the n50j model space and the NushellX@MSU code to methodically assess the function of core polarization in the ^{92}Mo nucleus. The improved concordance between our experimental results and theoretical form factors emphasizes how important it is to explicitly account for core polarization effects. Additionally, the observed differences at greater momentum transfers suggest that nuclear structure modeling may be improved, opening the door for further research that takes relativistic corrections and many-body effects into account.

4. Conclusion:

This work demonstrates that integrating core polarization (CP) effects is critical for greatly improving the agreement between theoretical form factor predictions and experimental observations across diverse nuclear states. The observed oscillatory behavior with greater momentum transfers indicates limits in the existing theoretical framework, needing additional development. Persistent disparities indicate that higher-order adjustments, such as many-body effects and relativistic contributions, are critical for improving prediction accuracy. Future research should concentrate on constructing more complete nuclear models that include these modifications, eventually improving our basic knowledge of nuclear structure and interactions.

Funding: None.

Data Availability Statement: All of the data supporting the findings of the presented study are available from corresponding author on request.

Declarations: **Conflict of interest:** The authors declare that they have no conflict of interest.

Ethical approval: This research did not include any human subjects or animals, and as such, it was not necessary to obtain ethical approval.

References

[1] Bohr and B. R. Mottelson. Nuclear structure. *Physics Today*, 2: 59–62, 1975, doi:10.1063/1.3037453.

[2] R. A. Silverman. *Scattering Theory for Particle Physics*. Dover Publications, New York, 1995.

[3] R. Hofstadter. Electron scattering and nuclear structure. *Reviews of Modern Physics*, 28: 214, 1956, doi:10.1103/RevModPhys.28.214.

[4] K.W. Ford and D.L. Hill. The distribution of charge in the nucleus. *Annual Review of Nuclear and Particle Science*, 5(1): 25, 1955, doi:10.1146/annurev.ns.05.120155.000325.

[5] T. W. Donnelly and J. D. Walecka. Electron scattering and nuclear electromagnetic response. *Annual Review of Nuclear and Particle Science*, 25: 329, 1975, doi:10.1146/annurev.ns.25.120175.001553.

[6] T. Forest, V. R. Pandharipande, and J. L. Friar. Electron scattering and nucleon correlations in nuclei. *Physical Review C*, 28: 756, 1983.

[7] T.W. Donnelly and J.D. Walecka. Elastic magnetic electron scattering and nuclear moments. *Nuclear Physics A*, 201:81, 1973, doi:10.1016/0375-9474(73)90689-1.

[8] J. Carlson. Quantum monte carlo calculations of light nuclei. *Reviews of Modern Physics*, 87: 1067, 2015, doi:10.1103/RevModPhys.87.1067.

[9] H. Beck and R. D. McKeown. Parity-violating electron scattering and strange quark contributions to the nucleon. *Annual Review of Nuclear and Particle Science*, 51: 189, 2001, doi:10.1146/annurev.nucl.51.101701.132312.

[10] F. A. Majeed. The effect of core polarization on longitudinal form factors in ^{10}B. *Physica Scripta*, 85: 065201, 2012, doi:10.1088/0031-8949/85/06/065201.

[11] F. A. Majeed and F. M. Hussain. The role of the core polarization on C2 and C4 form factors of fp-shell nuclei. *Romanian Journal of Physics*, 59: 95, 2014.

[12] F. A. Majeed and L. A. Najim. Contribution of high energy configurations to longitudinal and transverse form factors in p- and sd-shell nuclei. *Romanian Journal of Physics*, 89:611, 2015, doi:10.1007/s12648-014-0622-3.

[13] F. A. Majeed and S. M. Obaid. Nuclear structure study of ^{22,24}Ne and ^{24}Mg nuclei. *Revista Mexicana de Física*, 65:159, 2019.

[14] T. Iwamoto, H. Horie, and A. Yokoyama. Inelastic electron scattering form factors for the excitation of the 2+ states in the $1f_{7/2}$ nuclei. *Nuclear Instruments and Methods in Physics Research B*, 25: 658, 1982, doi:10.1103/PhysRevC.25.658.

[15] S. M. Obaid and F. A. Majeed. Longitudinal and transverse form factors from ^{65}Cu and ^{71}Ga nuclei. *Journal of the Korean Physical Society*, 82: 329, 2023, doi:10.1007/s40042-022-00682-w.

[16] B. A. Brown, R. Radhi, and B. H. Wildenthal. Electric quadrupole and hexadecupole nuclear excitations from the perspectives of electron scattering and modern shell-model theory. *Applied Radiation and Isotopes*, 101: 313, 1983, doi:10.1016/0370-1573(83)90001-7.

[17] R. A. Radhi, Z. A. Dakhil, and N. S. Manie. Microscopic calculations of quadrupole moments in li and b isotopes. *The European Physical Journal A*, 50, 2014, doi:10.1140/epja/i2014-14115-9.

[18] T. Deforest, Jr., and J.D. Walecka. Electron scattering and nuclear structure. *Radiochim Acta*, 15(57): 1, 1966, doi:10.1080/00018736600101254.

[19] J. Friedrich and P.-G. Reinhard. Skyrme-force parametrization: Least squares fit to nuclear ground-state properties. *Physical Review C*, 33: 335, 1990, doi:10.1103/PhysRevC.33.335.

[20] T. E. Milliman. *Inelastic Electron Scattering from Molybdenum-92*. PhD thesis, University of New Hampshire, 1987.

عوامل التشكل للأستطارة الالكترونية لـ ^{92}Mo في إطار إنموذج القشرة: دمج تأثيرات استقطاب القلب

سارة مهدي عبيد *

قسم الفيزياء الطبية، كلية العلوم، جامعة المستقبل، بابل، العراق.

* الباحث المسؤول: *sarah.mahdi@uomus.edu.iq*

الخلاصة

تم استخدام حسابات انموذج القشرة لدراسة عوامل التشكل الكولومية $C2$ و $C4$ والمستعرضة $E3$ و $E5$ و $E7$ ، مع تضمين تأثيرات استقطاب القلب في الحالات 2^+ ، 3^- ، $4+$ ، 5^- و 7^- لنواة ^{92}Mo . أجريت الحسابات باستخدام التفاعل الفعّال ثنائي الجسيمات $n50j$ مع فضاء الانموذج $n50j$. تم استخدام نموذج تاسي للتكافؤ الكولومي (*CVTM*) ،الذي يأخذ بنظر الاعتبار الإثارات خارج فضاء الانموذج، لتقييم تأثيرات استقطاب القلب .كما تم استخدام جهد سكيرم (*Skyrme potential*) لحساب دوال الموجة لعناصر المصفوفة أحادية الجسيمات الشعاعية، مما وفر وصفًا واقعيًا لتفاعلات النواة. تُعد تأثيرات استقطاب القلب أساسية في تحسين حسابات عوامل التشكل، حيث تؤدي إلى توافق أكبر مع البيانات التجريبية المتاحة.

الكلمات الدالة : عوامل التشكل $C2$ و $C4$ ، عوامل التشكل $E3$ و $E5$ و $E7$ ، نموذج تاسي، جهد سكيرم، استقطاب القلب.

التمويل: لايوجد.

بيان توفر البيانات: جميع البيانات الداعمة لنتائج الدراسة المقدمة يمكن طلبها من المؤلف المسؤول.

اقرارات:

تضارب المصالح: يقر المؤلفون أنه ليس لديهم تضارب في المصالح.

الموافقة الأخلاقية: لم يتضمن هذا البحث أي تجارب على البشر أو الحيوانات، بالتالي لم يكن من الضروري الحصول على موافقة أخلاقية.